THE JOURNAL OF BIOLOGICAL CHEMISTRY VOL. 286, NO. 11, pp. 9185–9195, March 18, 2011

Proprotein Convertase PC7 Enhances the Activation of the EGF Receptor Pathway through Processing of the EGF Precursor*[S]

Received for publication, September 29, 2010, and in revised form, December 17, 2010 Published, JBC Papers in Press, January 5, 2011, DOI 10.1074/jbc.M110.189936

Estelle Rousselet[‡], Suzanne Benjannet[‡], Edwidge Marcinkiewicz[‡], Marie-Claude Asselin[‡], Claude Lazure[§], and Nabil G. Seidah[‡1]

From the Laboratories of [‡]Biochemical Neuroendocrinology and [§]Neuropeptide Structure and Metabolism, Clinical Research Institute of Montreal, Montreal, Quebec H2W 1R7, Canada

Although the processing profile of the membrane-bound epidermal growth factor precursor (pro-EGF) is tissue-specific, it has not been investigated at the cellular level nor have the cognate proteinases been defined. Among the proprotein convertases (PCs), only the membrane-bound PC7, the most ancient and conserved basic amino acid-specific PC family member, induces the processing of pro-EGF into an ~115-kDa transmembrane form (EGF-115) at an unusual VHPR$^{290}\downarrow$A motif. Because site-directed mutagenesis revealed that Arg^{290} is not critical, the generation of EGF-115 by PC7 is likely indirect. This was confirmed by testing a wide range of protease inhibitors, which revealed that the production of EGF-115 is most probably achieved via the activation by PC7 of a latent serine and/or cysteine protease(s). EGF-115 is more abundant at the cell surface than pro-EGF and is associated with a stronger EGF receptor (EGFR) activation, as evidenced by higher levels of phosphorylated ERK1/2. This suggests that the generation of EGF-115 represents a regulatory mechanism of juxtacrine EGFR activation. Thus, PC7 is distinct from the other PCs in its ability to enhance the activation of the cell surface EGFR.

The type I membrane-bound epidermal growth factor precursor (pro-EGF)[2] is the prototypical and largest member (140–160 kDa) of the EGF-like family of growth factors, which also includes heparin binding-EGF, transforming growth factor α (TGFα), β-cellulin, neuregulins 1–4, epiregulin, epigen, cripto, and amphiregulin. Pro-EGF is highly expressed in the submaxillary gland, kidney, and lacrimal gland (1). EGF is known to induce cell survival, differentiation, and proliferation (2) by binding to its membrane-bound receptors (EGFRs) (3, 4). Although a wide variety of cancers express EGFR (5), clinical trials of EGFR inhibitors showed moderate beneficial effects (6). A better understanding of EGFR activation may lead to more rational approaches to drug development.

Processing of pro-EGF into the well known 53-amino acid (aa) mature mouse EGF after a basic residue both at the N- (Arg$^{959}\downarrow$) and C-terminal (Arg$^{1012}\downarrow$) ends is not equally efficient in various tissues. Thus, in the submaxillary gland, pro-EGF is fully and intracellularly processed by kallikreins into mature EGF and then stored in secretory granules (7). In contrast, in kidney, pro-EGF is found at the cell surface mainly as an unprocessed protein (1, 8) or as intermediate forms generated by unknown proteases (9–11). Among the processed forms in kidney, a prominent ~115-kDa membrane-bound intermediate (herein called EGF-115) was reported (12), as well as a soluble form in urine generated by an undefined serine protease (10).

Many of the estimated ~3500 mammalian secretory proteins, including growth factors and their receptors, are subjected to limited proteolysis by one or more of the nine members of the proprotein convertase (PC) family of serine proteinases of the subtilisin-kexin type as follows: PC1/3, PC2, Furin, PC4, PC5/6, PACE4, PC7, SKI-1/S1P, and PCSK9. Extensive biochemical and *in vivo* analyses expanded our understanding of some of the physiological functions of these PCs and their roles in embryonic development and in the adult. The first seven members cleave secretory proteins at specific single or paired basic aa within the motif (Arg/Lys)-(Xaa)$_n$-Arg$\downarrow$ (n = 0, 2, or 4 aa) (13–16). The last two members, SKI-1/S1P and PCSK9, do not cleave at basic aa and are major regulators of cholesterol and lipid metabolism (16, 17).

A number of investigations aimed at defining the sequence recognition of PCs revealed some degree of redundancy in their ability to process certain precursor proteins (18). Thus, both Furin and PACE4 redundantly process the TGFβ-like Nodal during early embryonic development (19). However, evidence for PC-specific substrates has also been presented. Thus, although Furin and PC5/6 often cleave the same substrates, the TGFβ-like growth differentiating factor GDF-11 is selectively cleaved by PC5/6 during development (20).

Although the physiological functions of most PCs are now better understood (16, 21), the unique functional roles of the seventh member PC7, the most ancestral of the basic aa-specific convertases, are barely explored. Although less efficient

* This research was supported by Canadian Institutes of Health Research Grant MOP-44363, a Strauss Foundation grant, and a Canada Chair Grant 216684.

[S] The on-line version of this article (available at http://www.jbc.org) contains supplemental Figs. S1–S5 and Tables S1 and S2.

[1] To whom correspondence should be addressed: Laboratory of Biochemical Neuroendocrinology, Clinical Research Institute of Montreal, 110 Pine Ave. West, Montreal, Quebec H2W 1R7, Canada. Tel.: 514-987-5609; E-mail: seidahn@ircm.qc.ca.

[2] The abbreviations used are: pro-EGF, EGF precursor; aa, amino acid; CT, cytosolic tail; dynasore, hydroxynaphthalene-2-carboxylic acid (3,4-dihydroxybenzylidene)-hydrazide monohydrate; EGF-115, ~115-kDa transmembrane EGF; EGFR, EGF receptor; endoH, endonuclease H; ER, endoplasmic reticulum; MβCD, methyl-β-cyclodextrin; nt, nucleotide; PC, proprotein convertase; TMCT, transmembrane-cytoplasmic; Tricine, *N*-[2-hydroxy-1,1-bis(hydroxymethyl)ethyl]glycine; h, human.

than Furin, PC7 specifically cleaves overexpressed substrates at Arg ↓ residues both *in vitro* (22–29) and in cell lines (30–39). Northern blot analyses revealed a wide expression of PC7 mRNA in all rat tissues and cell lines analyzed (40), suggesting that it may have multiple physiological functions. Quantitative RT-PCR analysis of PC7 expression in adult mouse tissues showed that colon, duodenum, heart, and kidney are the richest sources of PC7 mRNA (41).

We herein characterized the biosynthetic pathway of pro-EGF as well as its enhanced processing by PC7. Our data show that PC7 is the only convertase that enhances the indirect cleavage of pro-EGF into EGF-115, likely via the activation of serine and/or cysteine protease(s). We also show that EGF-115 is more concentrated at the cell surface and more efficiently activates the EGFR than full-length pro-EGF.

EXPERIMENTAL PROCEDURES

Plasmids and Reagents—All PCs constructions V5-tagged or not (mouse PC1, human Furin, mouse PC5/6A, human PACE4, full-length human PC7, full-length and soluble PC7 (PC7 and sPC7), rat PC7-KDEL, and rat PC7-GPI) were cloned into pIRES-2-GFP vector, as described previously (23, 31, 42). Mouse pro-EGF vector was purchased from ATCC (MGC-18573, GenBank™ BC017681.1) and subcloned with a 5′-Kozak sequence and a C-terminal V5 tag, into pIRES2-EGFP vector (Clontech). All of the oligonucleotides used in the various pro-EGF and PC7 constructions are listed in supplemental Tables S1 and S2.

In Situ Hybridization—Kidneys and lacrimal glands of adult wild type mice were frozen and cut into 10-μm sections. Tissue slices were fixed in 4% formaldehyde at 4 °C for 1 h. *In situ* hybridization was carried out as reported previously (43) using a complementary mouse pro-EGF or mouse PC7 cRNA probe (552 and 640 nucleotides (nts), respectively) labeled with ^{35}S-UTP. To generate a mouse pro-EGF cRNA probe, a cDNA segment covering the sequence encoding nts 3051–3602, localized downstream to mature EGF sequence, was PCR-amplified using sense 5′-GAAGCATGACATCATGGTGG-3′ and antisense 5′-GACACAGCTTATATATGAATGTCTTG-3′ oligonucleotides and subcloned into the vector pDrive (Invitrogen). To generate a mouse PC7 cRNA probe, a cDNA segment covering the sequence encoding amino acids 1–639 was amplified using sense 5′-TGCTGTTCTGATGCCGAAAGG-3′ and antisense 5′-GGGTCATTAGAGTTGAGGTCATAG-3′ oligonucleotides and subcloned into pCRII-TA cloning vector (Invitrogen). Hybridization was analyzed on x-ray film (exposure time, 2 days for EGF and 5 days for PC7).

Cell Culture and Transfections—HEK293, Neuro2A, COS-1, and A431 cell lines were grown in Dulbecco's modified Eagle's medium with 10% fetal bovine serum (Invitrogen) and were maintained at 37 °C under 5% CO_2. At 80–90% confluence, HEK293 cells were co-transfected in ratio of 1:1 with Effectene (Qiagen) and Neuro2A and COS-1 cells with Lipofectamine (Invitrogen) according to the manufacturer's instructions. Twenty four hours after transfection, the cells were washed and incubated in serum-free medium for an additional 20 h before medium collection and cell lysis. In some cases, 24 h post-transfection, cells were incubated overnight with either 2-bromopalmitate (2.5 or 25 μM, Sigma), decanoyl-RVKR-cmk (50 μM, Bachem), phospholipase C (0.5 units/ml, Sigma), or for various periods with cycloheximide (100 μM, Sigma).

Co-cultures—HEK293 cells expressing either pro-EGF, PC7, or pIRES were co-cultured at an EGF/PC7 cDNA ratio of 1:2. Twenty four hours later, the cells were washed and incubated overnight in serum-free medium before cell lysis. For co-cultures of HEK293 and A431 cells, 24 h post-transfection, HEK293 cells were trypsinized, and 4×10^5 cells were mixed in a new P3.5 plate containing 6×10^5 A431 cells. Twenty four hours later, the cells were washed and incubated in serum-free medium for 3 h before cell lysis. The incubation of this co-culture with mouse recombinant EGF (20 ng/ml) was used as a positive control for the phosphorylation of ERK1/2.

Immunoprecipitation and Western Blot Analysis—Cells were lysed in ice-cold precipitation assay buffer (50 mM Tris-HCl, pH 7.8, 150 mM NaCl, 1% Nonidet P-40, 0.5% sodium deoxycholate, 0.1% SDS) containing a mixture of protease inhibitors (Roche Applied Science). Proteins were analyzed by 8, 10, or 15% SDS-PAGE. For immunoprecipitation, cell lysates were incubated overnight at 4 °C with anti-V5-agarose (Sigma) or anti-streptavidin-agarose (Fluka) and washed five times with cold lysis buffer. Following addition of reducing Laemmli sample, solubilized proteins were separated by 8% SDS-PAGE. Proteins were visualized using rabbit anti-PC7 (1:10,000 (35)), mouse anti-Furin (1:2,000, MON148, Alexis), rabbit anti-PC1 (1:2,000 (44)), mouse anti-phospho-ERK1/2 (1:1,000, Cell Signaling), rabbit anti-ERK1/2 (1:1,000, Cell Signaling), rabbit anti-β-actin (1:5,000, Sigma), or a horseradish peroxidase (HRP)-conjugated mAb V5 (1:10,000, Sigma). Bound primary antibodies were detected with corresponding species, HRP-labeled secondary antibodies, and revealed by enhanced chemiluminescence. Quantitation of band intensity was done with Scion image software from the Scion Corp. (Frederick, MD).

Enzymatic Digestion of Carbohydrates—Proteins from cell lysates were incubated with endoglycosidase H (endoH) or *N*-glycosidase F for 1 h at 37 °C. Deglycosylated proteins were separated by 8% SDS-PAGE and revealed by immunoblotting.

Cell Surface Biotinylation—For biochemical detection of pro-EGF at the plasma membrane, transfected HEK293 cells were washed with ice-cold phosphate-buffered saline (PBS) adjusted to pH 8 and biotinylated with 0.2 mg of sulfosuccinimidyl-6-(biotin-amido) hexanoate (Pierce) for 30 min at 4 °C. Cells were then washed with 100 mM glycine in PBS, pH 8, to quench the reaction. Cell lysates were immunoprecipitated with anti-streptavidin-agarose (Fluka), and immunoprecipitates were then treated as described above.

Biosynthetic Analysis—HEK293 cells were transiently transfected in 60-mm dishes. Biosynthesis was performed 48 h post-transfection, and the cells were washed and pulse- labeled in Cys/Met-free RPMI 1640 medium containing 0.2% BSA for 2 h with 250 μCi/ml of [^{35}S]Cys/Met for all experiments except for sulfation of pro-EGF (2 h with 500 μCi/ml of $Na_2{}^{35}SO_4$). After the pulse, the media were recovered, and the cells were lysed as mentioned previously (45). For pro-EGF pulse-chase experiments, the cells were pulse-labeled with [^{35}S]Met/Cys for 20 min and then chased for various periods. The cell lysates were immunoprecipitated with mAb V5 (1:500, Invitrogen). The

immunoprecipitated proteins were resolved by SDS-PAGE on 8% Tricine gels, dried, and autoradiographed, as described previously (45). In some cases, during the 30 min preincubation times for pulse analysis, the cells were pretreated with brefeldin A (2.5 μg/ml, Calbiochem), methyl-β-cyclodextrin (MβCD, 10 mM, Sigma), or 3-hydroxynaphthalene-2-carboxylic acid (3,4-dihydroxybenzylidene)-hydrazide monohydrate (Dynasore; 80 μM, Sigma), and this treatment was continued during the 2-h pulse period. Protease inhibitors were added during the 2-h pulse period. The concentrations used, listed in Table 1, were based on previous reports (46–53). Half of the cellular proteins were precipitated with mAb V5 (1:500, Invitrogen) and the other half with rabbit anti-PC7 (10 μl (35)).

N-terminal Microsequencing Analysis of EGF-115-kDa Form—Transiently transfected HEK293 cells were pulse-labeled for 4 h with 250 μCi/ml [^{35}S]Met (Amersham Biosciences). Lysates were immunoprecipitated with mAb V5 (1:500, Invitrogen), and proteins were resolved by SDS-PAGE on 8% Tris-Tricine gel, immobilized to PVDF membrane (Millipore). The radiolabeled EGF-115-kDa form was excised and microsequenced as described previously on an Applied Biosystems Procise cLC protein sequencer (45).

Fluorescence-activated Cell Sorting (FACS)—Twenty four hours post-transfection, HEK293 cells were processed for flow cytometry. Cells were washed with buffer A (1× PBS with 7.1 ml of 35% BSA and 2 ml of 250 mg/liter glucose) and then stained with a rat anti-mouse pro-EGF primary antibody (1:250, R&D Systems) for 40 min at room temperature and then with anti-rat IgG conjugated with Alexa 647 (1:750, Molecular Probes) for 20 min at room temperature. FACS analysis was performed using the CyAn ADP cytometer (Beckman Coulter), and the data were analyzed using the Summit software (Beckman Coulter). The mean fluorescence intensity of EGF at the cell surface for a population of 50,000 cells was determined.

Immunofluorescence—Cells were plated on collagen-coated culture dishes (MatTek) and then transfected the following day. Twenty four hours post-transfection, the cells were fixed for 15 min with 4% paraformaldehyde + 1% methanol for PC7 and pro-EGF cell surface labeling to slightly permeabilized cell to have access to the V5 tag or 5 min at −20 °C with 100% methanol for intracellular staining. Cell fixed with paraformaldehyde were incubated 5 min in 150 mM glycine to quench aldehyde groups. Cells were then incubated overnight with primary antibodies. PC7 was detected with rabbit anti-PC7 (1:1,000 (35)) and pro-EGF with mAb V5 (1:200, Invitrogen). Antigen-antibody complexes were revealed by 1 h of incubation with the corresponding species-specific Alexa Fluor (488, 555, or 647)-tagged antibodies (Molecular Probes), and the nuclei were stained by Hoechst 33258 for 1 min (100 μg/ml, Sigma). Cells were covered with 1,4-diazabicyclo[2.2.2]octane (Sigma) in PBS, 90% glycerol, and immunofluorescence analyses were performed with a confocal microscope (Zeiss LSM-710).

In Vitro Activity Assay—Enzymatic *in vitro* assays were performed in 100 μl of buffer (1 mM $CaCl_2$, 25 mM Tris-HCl, pH 6.7) at 37 °C for 1 h in the presence of 100 μM of the substrate pyroglutamic acid-RTKR-7-amido-4-methylcoumarin (23) and 5 μl of concentrated media from HEK293 cells expressing either sPC7 or pIRES. The media were first preincubated for 20 min with the protease inhibitors, and then the fluorogenic substrate was added for a further incubation of 1 h. The release of free 7-amino-4-methylcoumarin was detected with a spectra MAX GEMINI EM microplate spectrofluorimeter (Molecular Devices, excitation, 360 nm; emission, 460 nm). The mean of the relative fluorescence unit of three independent experiments is reported.

Statistical Analysis—All experiments were performed at least in triplicate. Quantifications are defined as mean ± S.E. In some cases, results were expressed as percentage of control, which was considered to be 100% or normalized to EGF + pIRES, which was considered as 1. The statistical significance of differences between various groups was evaluated by one-way analysis of variance test followed by the Dunnet test. A difference between experimental groups was considered statistically significant whenever the p value was <0.05.

RESULTS

PC7 Processes Pro-EGF into an ~115-kDa Membrane-bound Form—We first tested the possible implication of PCs in the processing of the cell surface pro-EGF, which may mimic the undefined kidney protease reported to be implicated in pro-EGF maturation (12). Thus, we co-expressed pro-EGF in HEK293 or Neuro2A cells with PC1/3, Furin, PC5/6A, PACE4, or PC7, the only basic aa-specific PCs that can function in the *trans*-Golgi network and/or cell surface (16). The data demonstrated that under our experimental conditions, in the two cell lines, only PC7 significantly processed (~45%) the membrane-bound pro-EGF, resulting into an ~115-kDa nonsecreted V5-tagged product (EGF-115; Fig. 1*A*). In addition, no smaller cellular V5-tagged fragment(s) was detected in cells (data not shown), suggesting that pro-EGF is not shed into the HEK293 media. To check and compare the protein levels of the overexpressed PCs, V5-tagged PCs, except for PC1 that was detected with a C-terminal PC1-specific antibody (44), were co-expressed in HEK293 cells. The data show that all PCs are similarly expressed (supplemental Fig. S1). This conclusion was further supported by the analysis of the EGF immunoreactivity in the media, which showed that no PC can generate the 53-aa mature EGF or any shed form of pro-EGF (supplemental Fig. S2). Intriguingly, we also noted that in COS-1 cells PC7 was much less efficient in generating EGF-115 because the cleavage of pro-EGF represented only ~25% compared with ~45% in Neuro2A and HEK293 cells (Fig. 1*A*). We confirmed that the PC7 activity is necessary for the observed pro-EGF processing by treating cells with the general PC inhibitor decanoyl-RVKR-cmk (Fig. 1*B*) (42), which resulted in much reduced levels of EGF-115 similar to basal levels (~14%). It is thus possible that the EGF-115-like band seen in the absence of overexpressed PC7 may not be exclusively PC7-generated. This is supported by the treatment of Neuro2A cells with an siRNA against PC7, which completely abolished endogenous PC7 expression but the background EGF-115-like band still remained (supplemental Fig. S3).

In situ hybridization of pro-EGF and PC7 mRNA showed that whereas lacrimal glands express high levels of pro-EGF, they only exhibit low levels of PC7 transcripts (Fig. 2). In contrast, both are highly expressed and co-localized in the medulla

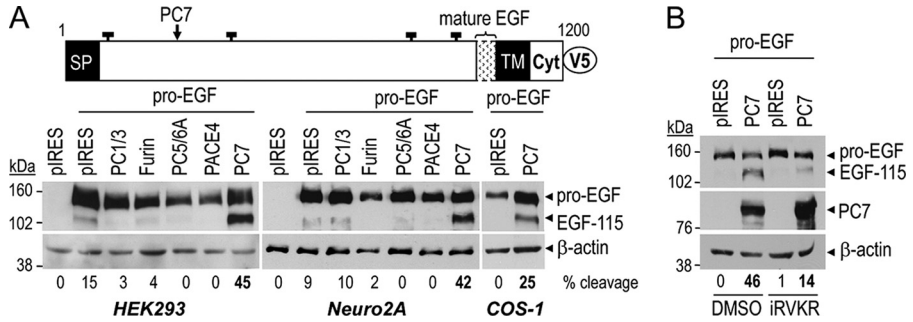

FIGURE 1. **Pro-EGF is processed only by PC7 into EGF-115.** *A,* schematic diagram depicting pro-EGF and Western blot analysis of lysates from cells expressing pro-EGF-V5 and diverse basic aa-specific PCs in HEK293 and Neuro2A cells and with PC7 in COS-1 cells. Cell lysates were separated on 8% SDS-PAGE, and pro-EGF-related proteins revealed by Western blot using mAb V5 and loading were estimated with β-actin antibody. *B,* Western blot analysis of lysates from cells expressing pro-EGF-V5 and either PC7 or an empty vector (*pIRES*). Cells were incubated for 16 h with either 0.1% dimethyl sulfoxide (DMSO, control) or with 50 μM of the PC inhibitor decanoyl-RVKR-cmk (*iRVKR*) dissolved in 0.1% DMSO. Separated cellular proteins were revealed by Western blot using mAb V5-HRP (pro-EGF), PC7, or β-actin antibodies. The percent of pro-EGF cleavage into EGF-115 is indicated *below* each lane. These data are representative of at least three independent experiments.

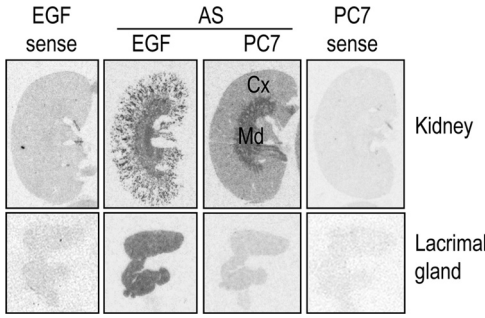

FIGURE 2. **Localization of PC7 and EGF mRNAs in mouse kidney and lacrimal gland.** *In situ* hybridization on cryosections in adult mouse kidney and lacrimal gland with a PC7 and EGF antisense (*AS*) and control sense ^{35}S-labeled cRNA probes. *Cx,* cortex; *Md,* medulla.

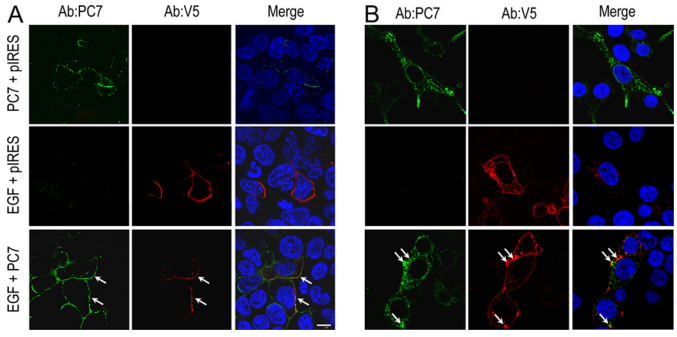

FIGURE 3. **Co-localization of pro-EGF and PC7 in HEK293 cells.** Pro-EGF and PC7 immunocytochemical staining under slightly permeabilizing conditions (*A*) and permeabilizing conditions (*B*), using a polyclonal PC7 antibody (*green labeling*) and mAb V5 for pro-EGF staining (*red labeling*). Nuclei of transfected cells are marked by Hoechst 33258 staining (*blue labeling*). Co-localization areas are exemplified by *arrows* and by *yellow color* in the *merged image*. *Bar,* 10 μm. These data are representative of at least three independent experiments.

and cortex of the kidney (Fig. 2). Because kidney pro-EGF is cleaved into an EGF-115-like product (12), the above data suggest that PC7 may be involved in pro-EGF processing in the kidney. Furthermore, in HEK293 cells, pro-EGF and PC7 co-localize at the cell surface under slightly permeabilizing conditions (Fig. 3*A*) and in subcellular compartments just under the cell surface under permeabilizing conditions (Fig. 3*B*). Altogether, these data support the hypothesis that PC7 may process pro-EGF *ex vivo* and likely *in vivo* into EGF-115.

Generation of EGF-115 Requires Endocytosis and Cholesterol-rich Microdomains—Because pro-EGF and PC7 are highly expressed in the kidney and co-localize in HEK293 cells, all subsequent experiments were performed in the latter cells. To define the processing kinetics and the compartment(s) where such cleavage occurs, cells expressing PC7 and pro-EGF were pulsed with [^{35}S]Met/Cys for 20 min and then chased for 1–5 h, followed by SDS-PAGE analysis of the cell lysates immunoprecipitated with the mAb V5 (Fig. 4*A*). Although EGF-115 was not detected at 30 min (data not shown), it appeared by 1 h and reached maximum levels by 2 h of chase, followed by a slow decline, suggesting that processing occurs after pro-EGF exits from the endoplasmic reticulum (ER). Indeed, pro-EGF is partially sensitive to endoH digestion (Fig. 4*B*), and only ~50% of it, compared with [^{35}S]Met/Cys-labeling, is sulfated (Fig. 4*C*), suggesting that only the latter fraction exited the ER. In contrast, EGF-115 is both endoH-insensitive (Fig. 4*B*) and is fully sulfated (Fig. 4*C*), supporting the notion that it is produced in a post-ER compartment.

We next tested whether retention of pro-EGF and/or PC7 in the ER would permit processing. Thus, HEK293 cells expressing pro-EGF and PC7 were incubated with brefeldin A, which inhibits ER to Golgi transport of proteins (54). This treatment prevented pro-EGF processing because it reduced the level of EGF-115 to the basal one (~14%). (Fig. 4*D*). Similarly, a PC7-KDEL construct, which retains the enzyme in the ER because of its C-terminal KDEL sequence (55), cannot process pro-EGF (Fig. 4*E*). We conclude that processing of pro-EGF does not occur in the ER but rather in a post-ER compartment.

To further identify such a compartment, we tested the implication of cholesterol-rich microdomains or endosomes as follows. 1) Accordingly, we first evaluated whether depletion of the cholesterol cell content would affect the ability of PC7 to generate EGF-115 from pro-EGF. The extraction of cholesterol was achieved with MβCD that has been shown to selectively eliminate cholesterol from the plasma membrane, in preference to other lipids (56). Thus, cells expressing pro-EGF and either pIRES or PC7 were preincubated with 10 mM MβCD for 30 min and then radiolabeled for 2 h with [^{35}S]Met/Cys in the presence of the same cholesterol-depleting agent. This treatment completely abrogated the generation of EGF-115 (Fig.

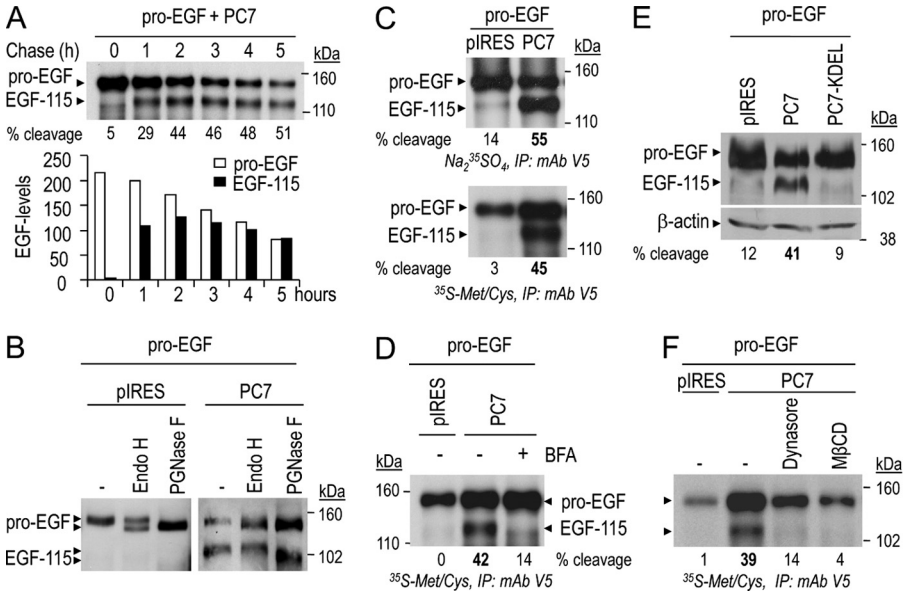

FIGURE 4. **EGF-115 form is processed by PC7 in lipid-rich post-ER compartment after clathrin-dependent endocytosis.** *A,* pulse-chase analysis of pro-EGF and its EGF-115 fragment obtained by co-expressing pro-EGF and PC7 in HEK 293 cells pulse-labeled with [^{35}S]Met/Cys for 20 min and chased for 1–5 h in the absence of radiolabel. The proteins were immunoprecipitated with mAb V5, and the SDS-PAGE-separated proteins were quantitated from the autoradiogram by Scion image analysis, and the data are presented in a *bar graph* format. *B,* treatment with endoH and *N*-glycosidase F (*PGNase F*) of lysates of HEK293 cells co-expressing pro-EGF and either pIRES or PC7. The Western blot shows that pro-EGF is partially sensitive to endoH digestion, whereas EGF-115 is totally resistant to endoH. *C,* $Na_2{}^{35}SO_4$ or [^{35}S]Met/Cys labeling for 2 h of HEK293 cells co-expressing pro-EGF and either pIRES or PC7. Cell lysates were immunoprecipitated (*IP*) with mAb V5 and then run on a 8% SDS-PAGE. *D,* autoradiograph of pro-EGF using mAb V5 of proteins extracted from HEK293 cells co-expressing pro-EGF and either pIRES or PC7, pulse-labeled with [^{35}S]Met/Cys, and treated or not with 2.5 μg/ml brefeldin A (*BFA*). Cell lysates were immunoprecipitated with mAb V5 and then run on a 8% SDS-PAGE. *E,* Western blot analysis of cells co-expressing pro-EGF with either pIRES, PC7, or PC7-KDEL reveals that pro-EGF processing does not occur in the ER. *F,* autoradiograph of cell lysates of HEK293 cells co-expressing pro-EGF and either pIRES or PC7, pulse-labeled with [^{35}S]Met/Cys, and incubated with Dynasore (80 μM) or MβCD (10 mM). The percent of pro-EGF cleavage into EGF-115 is indicated *below* each lane. These data are representative of three independent experiments.

4*F*). These data suggest that processing of pro-EGF requires the presence of cholesterol-rich microdomains. 2) Incubation of the same cells with 80 μM dynasore, a cell-permeable inhibitor of dynamin GTPase activity that blocks clathrin-dependent endocytosis (57), also reduced to basal levels (~14%) the generation of EGF-115 (Fig. 4*F*). 3) Finally, the requirement of endocytosis for pro-EGF processing is supported by the lack of generation of EGF-115 in confluent co-cultures of pro-EGF-expressing cells with those expressing either PC7 or its soluble secretable form sPC7 (supplemental Fig. S4). These data suggest that pro-EGF processing by full-length membrane-bound PC7 does not occur at the cell surface, but rather it requires endocytosis of pro-EGF into clathrin-coated pits and likely localization in cholesterol-rich microdomains.

Transmembrane Full-length PC7 Can Process Membrane-bound and Soluble Pro-EGF—Interestingly, the transmembrane (TM)-cytoplasmic (CT) domains of pro-EGF are dispensable, because PC7 can process both wild type (WT) and soluble pro-EGF (Fig. 5*A*). However, soluble sPC7 cannot process WT pro-EGF (Fig. 5*B*), although sPC7 is active in *in vitro* assays (23). These data suggested that the TMCT domain of PC7 is required for pro-EGF processing.

PC7 is the only convertase that contains Cys-palmitoylation sites within its cytosolic domain (Fig. 6*A*) (41, 58). Thus, we tested whether the CT-Cys-palmitoylation regulates pro-EGF processing. We note that both human and rat CTs contain five and eight Cys residues, respectively. Earlier work indicated that in h-PC7, Cys^{699} and Cys^{704} are palmitoylated (58), and our [^{3}H]palmitate incorporation studies with the double PC7

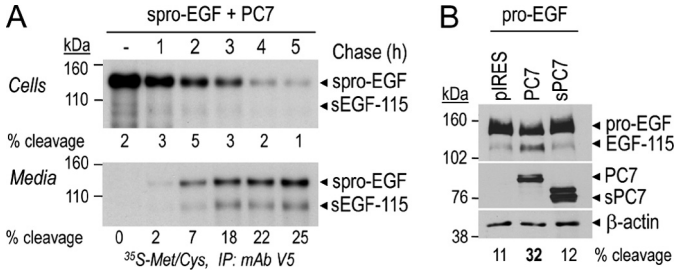

FIGURE 5. **Transmembrane and cytosolic domain of pro-EGF is dispensable for PC7 activity whereas that of PC7 is not.** *A,* HEK293 cells co-expressing PC7 and soluble pro-EGF (*spro-EGF*) were pulsed with [^{35}S]Met/Cys for 30 min and chased in the absence of label for 1–5 h. The cell lysates and media were then immunoprecipitated with mAb V5, and the proteins were separated by 8% SDS-PAGE. The dried gel was then autoradiographed for 6 h. Note that the estimated half-life of soluble pro-EGF is ~1 h. *B,* Western blot analysis of lysates of HEK293 cells co-expressing pro-EGF and either pIRES, full-length PC7, or its soluble form (*sPC7*). The separated proteins were revealed using mAb V5-HRP, PC7, or β-actin antibodies. The percent of pro-EGF cleavage into EGF-115 is indicated *below* each lane. These data are representative of three independent experiments.

mutant C699A,C704A confirmed that these are the only palmitoylation sites in h-PC7 when expressed in HEK293 cells (41). Both WT and PC7-(C699A,C704A) double mutant process pro-EGF equally well (~47%, Fig. 6*B*). In addition, 2-bromopalmitate, a palmitoylation inhibitor, does not prevent pro-EGF processing by PC7 (Fig. 6*C*). Altogether, these data demonstrate that Cys-palmitoylation is not required for PC7 activity on pro-EGF.

To determine whether specific sequences within the TM or TMCT domains of PC7 are critical for its activity on pro-EGF,

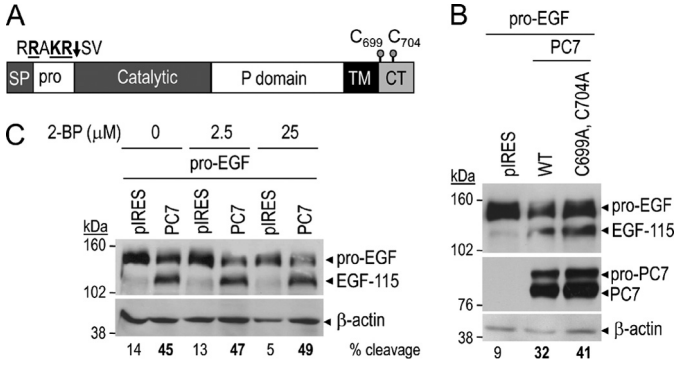

FIGURE 6. **Effect of Cys-palmitoylation on PC7 activity.** *A,* schematic diagram depicting pro-PC7, in which the autocatalytic cleavage site of the prosegment and cytosolic tail palmitoylated Cys^{699} and Cys^{704} are emphasized. *SP,* signal peptide, *Pro,* prosegment, *TM,* transmembrane domain, *CT,* cytoplasmic tail. *B,* Western blot analysis of pro-EGF, PC7, and β-actin in cells co-expressing pro-EGF and either wild type PC7 or nonpalmitoylated PC7-(C699A,C704A) double mutant. *C,* Western blot analysis of pro-EGF and β-actin in cells expressing pro-EGF and PC7 treated or not with 2.5 or 25 μM of 2-bromopalmitate (*2-BP*). The percent of pro-EGF cleavage into EGF-115 is indicated *below* each lane. These data are representative of three independent experiments.

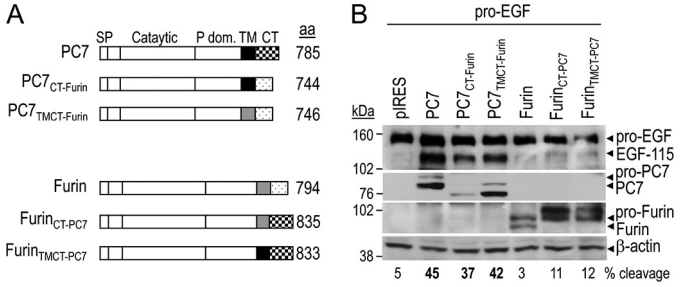

FIGURE 7. **Transmembrane and cytosolic domain of PC7 can be replaced by that of Furin.** *A,* schematic diagrams depicting chimeras of PC7 and Furin. *B,* Western blot analysis of lysates of cells expressing pro-EGF and either pIRES, PC7, its chimeras $PC7_{CT\text{-}Furin}$, $PC7_{TMCT\text{-}Furin}$, Furin, or its chimeras $Furin_{CT\text{-}PC7}$ and $Furin_{TMCT\text{-}PC7}$. Immunoreactive proteins were revealed using mAb V5-HRP (pro-EGF), PC7, Furin, or β-actin antibodies. The percent of pro-EGF cleavage into EGF-115 is indicated *below* each lane. These data are representative of three independent experiments.

we swapped these domains in h-PC7 with the corresponding ones of h-Furin ($PC7_{CT\text{-}Furin}$; $PC7_{TMCT\text{-}Furin}$) and vice versa ($Furin_{CT\text{-}PC7}$ and $Furin_{TMCT\text{-}PC7}$) (Fig. 7*A*) (41). None of these swaps affected the extent of PC7-processed pro-EGF, which is maintained at ~47%, or allowed cleavage of pro-EGF by Furin (Fig. 7*B*). Thus, although pro-EGF processing requires a membrane-bound form of PC7, the TMCT of the latter can be replaced by that of Furin.

PC7 Indirectly Enhances the Processing of Pro-EGF at VHPR^{290}—Because Leu is an abundant aa within the pro-EGF sequence, we tried to microsequence the [^{3}H]Leu-labeled EGF-115. However, our multiple attempts failed to give a clear protein sequence (data not shown). This may be due to the absence of Leu within the first 20 residues of the EGF-115 or to the presence of a Gln early in the sequence that would cyclize and block sequencing.

To identify the pro-EGF cleavage site, we generated various secretory pro-EGF deletants by fusing the signal peptide to either aa 160, 202, 310, or 341 (Fig. 8*A*) and estimated their molecular mass compared with the EGF-115 (Fig. 8*B*). The data showed that cleavage seems to occur close to the $LKQR^{310}$ site (Fig. 8*B*). However, systematic mutations of Arg around this site in mouse pro-EGF, including the mutants R294A, R310A, R312A, R315A, R321A, did not affect processing (data not shown). Because microsequencing did not yield informative results, we suspected that cyclization of a Gln may have hindered sequencing by Edman degradation. Accordingly, among other mutants, we concentrated on the double mutant Q292M,K300M because Lys^{300} is not conserved, and the specific activity of [^{35}S]Met is much higher than that of [^{3}H]Leu. Microsequencing of [^{35}S]Met-labeled EGF-115 resulting from the pro-EGF-(Q292M,K300M) double mutant gave a clear sequence with a Met at positions 2 and 10. This unique sequence unambiguously identified Arg^{290} as the cleavage site, pointing to an unusual processing motif $VHPR^{290} \downarrow A$ (Fig. 8*C*), which is not a normal cleavage site for any PC, as it does not display a second basic residue preceding Arg^{290} (13). It was thus not surprising that the R290A mutation did not affect processing of pro-EGF, which is maintained at ~50% (Fig. 8*D*). This suggests that PC7 triggers the cleavage activation of an unknown latent protease, which then cleaves pro-EGF at Arg^{290}. Furthermore, the PC7 dose-dependent processing of pro-EGF was not sensitive to PC7 levels between 3 and 300 ng of cDNA transfected, for a constant level of pro-EGF cDNA of 300 ng. This represents a similar efficacy of processing for PC7/EGF cDNA ratios of 1:1 up to 1:100 (Fig. 8*E*), suggesting that the level of the latent protease is limiting, and a small amount of PC7 activity, inhibitable by dec-RVKR-cmk (Fig. 1*B*), is enough to activate it. We also presume that the low efficacy of pro-EGF processing in COS-1 cells (Fig. 1*A*) may be due to an even lower level of the cognate latent enzyme in the latter cells *versus* HEK293 or Neuro2A cells.

To define the nature of the intermediate protease, we first tested the effect of a wide range of protease inhibitors on pro-EGF processing. HEK293 cells co-expressing pro-EGF and either pIRES or PC7, pulse-labeled with [^{35}S]Met/Cys, were incubated with different protease inhibitors (Table 1). Our data showed that the membrane-permeable cysteine protease inhibitor (2*S*,3*S*)-*trans*-epoxysuccinyl-L-leucylamido-3-methylbutane ethyl ester (E64d, 25 μM) and the serine protease inhibitors 4-(2-aminoethyl) benzenesulfonyl fluoride hydrochloride (AEBSF, 300 μM) and α_1-antitrypsin (0.5 mg/ml) significantly decreased (60–70%) the processing of pro-EGF into EGF-115 (Fig. 9*A*). These inhibitors did not inactivate PC7 *in vitro* even at high concentrations (Fig. 9*B*). Altogether these data suggest that the intermediate enzyme is either a cysteine and/or serine protease or that PC7 concomitantly activates cysteine and/or serine proteases. All other protease inhibitors had no significant effect on pro-EGF processing (Fig. 9, *A* and *C*). The presence of a proline in P2 is unusual and raised the possibility that thrombin, granzyme M, or neurolysin (59, 60) may be the intermediate enzyme. We thus tested the importance of this proline by mutagenesis (P289A). The cleavage of pro-EGF into EGF-115 represented ~45% even with pro-EGF mutant P289A, demonstrating that the proline in P2 is not critical for the intermediate enzyme (Fig. 9*D*). Furthermore, treatment of HEK293 cells co-expressing pro-EGF and PC7 with specific thrombin (antithrombin III) and neurolysin (Pro-Leu) inhibitors had no effect on pro-EGF processing (Fig. 9*A*).

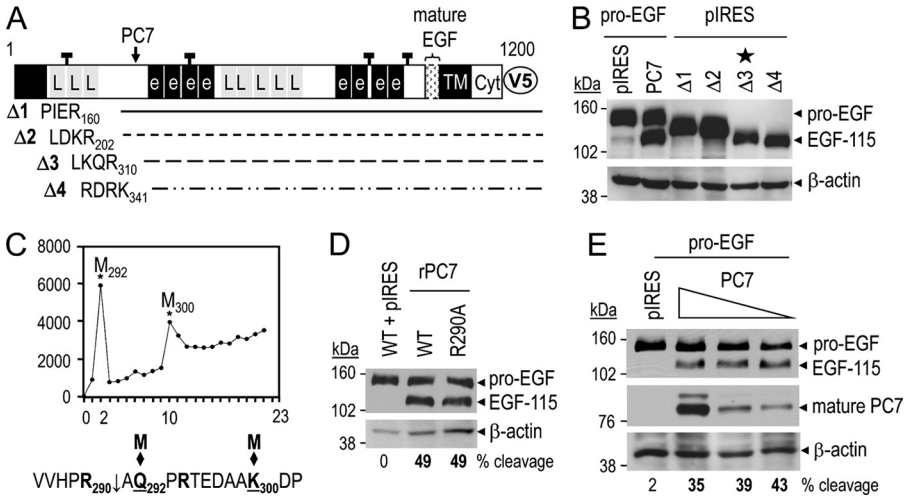

FIGURE 8. **Identification of the pro-EGF cleavage site.** *A,* schematic representation of mouse pro-EGF and the generation of deletants of mouse pro-EGF. The *arrow* points to the position of the pro-EGF cleavage site in presence of PC7. The exact positions of the deleted fragments generated are indicated with their C-terminal sequence. *e*, EGF like-repeat domains; *L*, LDL receptor class B repeats, and putative *N*-glycosylation sites are represented by *dark rectangles*. *B,* cells expressing pro-EGF with either pIRES or PC7 or pIRES together with deleted pro-EGF constructs. Western blot analysis of pro-EGF with mAb V5 shows the migration positions of the different constructs. *C,* microsequencing of the [^{35}S]Met-labeled pro-EGF-(Q292M,K300M) double mutant obtained from cell lysates. The deduced sequence positions of the ^{35}S-radiolabeled residues are shown. *D,* processing of pro-EGF or its R290A mutant into EGF-115 in the absence or presence of rat PC7 was tested as described above. *E,* Western blot of lysates obtained from cells expressing pro-EGF (300 ng) and three different doses of PC7 (300, 30, and 3 ng) shows that pro-EGF processing requires less than 100-fold lower cDNA input of PC7 compared with pro-EGF. The percent of pro-EGF cleavage into EGF-115 is indicated *below* each lane. These data are representative of three independent experiments.

TABLE 1
Concentration of protease inhibitors

Protease class inhibitor	Final concentration	Company
Metalloproteases		
EDTA-Na_2	200 μM	Roche Applied Science
Phosphoramidon	10 μM	Roche Applied Science
GM6001	25 μM	Calbiochem
Serine and cysteine proteases		
Antipain	50 μM	Roche Applied Science
Leupeptin	100 μM	Roche Applied Science
EST/E64d	25 μM	Calbiochem
AEBSF (Pefabloc SC)	300 μM	Roche Applied Science
α_1-Antitrypsin, human plasma	0.5 mg/ml	Calbiochem
Aprotinin	10 μM	Roche Applied Science
Chymostatin	100 μM	Roche Applied Science
Nafamostat	10^{-7} M	Sigma
GPI anchor Phospholipase C	0.5 unit/ml	Sigma
Thrombin Antithrombin III, human plasma	10 μg/ml	Calbiochem
Aspartic proteases		
Pepstatin A	1 μM	Roche Applied Science
Amino peptidases		
Bestatin	50 μM	Roche Applied Science
Neurolysin		
H-pro-Leu-OH	50 mM	Bachem

EGF-115 Exhibits Higher Cell Surface Localization and Activity on EGFR than Pro-EGF—To increase the level of the EGF-115, we generated an RRRR^{290}EL mutant at the PC7-enhanced cleavage site (Fig. 10*A*) exhibiting an optimal Furin-like motif, which would be expected to be cleaved efficiently by endogenous PCs in HEK293 cells (61). Indeed, although EGF-115 represents ~40% of total wild type pro-EGF indirectly produced by PC7, its level rises to ~55% in the RRRR^{290}EL mutant (Fig. 10*A*). Accordingly, we compared the cell surface expression of pro-EGF and pro-EGF co-expressed with PC7 with that of the RRRR^{290}EL mutant by FACS (Fig. 10*B*), cell surface biotinylation (Fig. 10*C*), and immunocytochemistry (Fig. 10*D*) analyses. The FACS experiment showed that although the number of cells expressing cell surface pro-EGF was similar in all transfections (data not shown), the mean cell surface fluorescence intensity of pro-EGF significantly increased ~1.7-fold in the RRRR^{290}EL mutant (Fig. 10*B*). Interestingly, immunohistochemistry shows a clear enrichment of pro-EGF at the cell surface in pro-EGF-(RRRR^{290}EL)-overexpressing cells (Fig. 10*D*). Finally, in the presence of PC7, cell surface biotinylation data show that EGF-115 is the major cell surface protein (~66% of total cell surface pro-EGF) as compared with pro-EGF (Fig. 10*C*).

Cycloheximide treatment of HEK293 cells overexpressing pro-EGF and PC7 showed that the levels of pro-EGF and its EGF-115 derivative were stable during the first 4 h of treatment. Following this initial period, they were both degraded with similar kinetics of ~7% decrease/hour with estimated half-lives of ~8–9 h (Fig. 10*E*). We conclude that the increased presence of the EGF-115 at the cell surface is not due to a longer half-life *versus* pro-EGF but rather to a preferred localization of this product at the cell surface, which may thus enhance activation of the EGFR.

To verify this hypothesis, we analyzed EGFR activation via the downstream phosphorylation of the MAPK ERK1 and ERK2 (62). Transfected HEK293 cells were mixed with A431 cells, known to express high levels of EGFR (63), and hence represent better responders to EGF. The amount of phosphorylated and nonphosphorylated ERK1/2 was estimated by Western blotting (Fig. 10*F*). We demonstrate that cells co-expressing pro-EGF and an empty vector (control) or sPC7 induce a low level of ERK1/2 phosphorylation (Fig. 10*F*). In contrast, co-expression of pro-EGF with PC7 or expression of the pro-EGF-RRRR^{290}EL mutant induce a higher level of ERK1 phosphorylation (~2- and ~5-fold increase, respectively) than cells

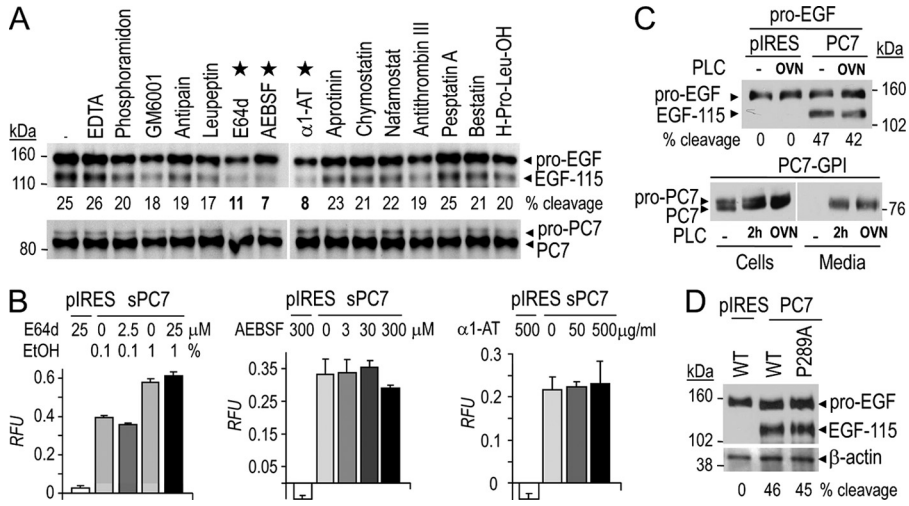

FIGURE 9. **Pro-EGF is processed by PC7 via serine and/or cysteine proteases.** *A,* HEK293 cells co-expressing PC7 and pro-EGF were pulse-labeled with [^{35}S]Met/Cys for 2 h and treated with a wide range of protease inhibitors. Half of the cell lysates were immunoprecipitated with mAb V5 and the other half with rabbit anti-PC7. Proteins were separated by 8% SDS-PAGE, and corresponding dried gels were autoradiographed for 3 h (immunoprecipitation (*IP*) with mAb V5) or 1 h (immunoprecipitation with Ab/PC7). *B, in vitro* enzymatic assays of PC7 and control from conditioned media of HEK293 cells expressing sPC7 or pIRES. The fluorogenic substrate used was pyroglutamic acid-RTKR-7-amido-4-methylcoumarin in the presence or absence of different concentrations of (2*S*,3*S*)-*trans*-epoxysuccinyl-L-leucylamido-3-methylbutane ethyl ester (*E64d*), 4-(2-aminoethyl) benzenesulfonyl fluoride hydrochloride (*AEBSF*), or α_1-antitrypsin (*α1-AT*). No significant inhibition of PC7 was achieved with either inhibitor (analysis of variance test). *RFU*, relative fluorescent units. *C,* Western blot analysis of lysates and media from cells expressing pro-EGF and either PC7 or pIRES and as positive control PC7-GPI and incubated or not with 5 units/ml of phospholipase C for 2 h or overnight. Separated cellular proteins were revealed by Western blot using mAb V5-HRP or PC7 antibodies. The percent of pro-EGF cleavage into EGF-115 is indicated *below* each lane. These data are representative of three independent experiments. *D,* Western blot analysis of lysates from HEK293 cells expressing pro-EGF-V5 or its P289A mutant with pIRES or PC7. Cell lysates were separated on 8% SDS-PAGE and proteins revealed by Western blot using mAb V5-HRP and loading was estimated with a β-actin antibody.

co-expressing pro-EGF and pIRES (control). ERK2 phosphorylation was also increased but was detected at very low levels. Collectively, these data demonstrate that PC7 processing favors the cell surface localization of EGF-115, and consequently it enhances EGFR activation.

DISCUSSION

Although EGF has strong biomedical significance, little is known about its biosynthesis and processing, especially the enzymes responsible for the soluble and transmembrane intermediate EGF forms (9, 10). Here, we examined the possible implication of the proprotein convertases in pro-EGF maturation. The data showed that none of the basic aa-specific PCs were able to generate soluble EGF forms in media, including the 53-aa EGF hormone (supplemental Fig. S2), suggesting that the serine protease involved in release of soluble EGF (10) is not a member of PC family. However, we did find that only full-length membrane-bound PC7 can enhance the processing of pro-EGF into an intermediate ~115-kDa transmembrane form (EGF-115; Fig. 1), which had already been observed in kidney, but not in lacrimal gland, extracts (12). Interestingly, we demonstrate that in kidney both PC7 and EGF mRNAs are abundant, but PC7 expression is very low in lacrimal glands (Fig. 2), in which EGF is only stored as its full-length membrane precursor (12). Thus, the low level of PC7 in lacrimal glands may explain the absence of EGF-115 in this tissue. We also showed that PC7 co-localizes with pro-EGF in HEK293 cells (Fig. 3). These data support the notion that PC7 induces pro-EGF processing *ex vivo* and may play the same function *in vivo*.

The proprotein convertase PC7, the most ancient and conserved PC-like enzyme, is the least studied member of the mammalian basic aa-specific PCs. When it was first discovered in 1996 (40, 64), it was thought to have similar properties to the other members of the family in terms of its zymogen activation, cellular trafficking, and cleavage specificity (23, 32). Although Furin knock-out mice exhibited early embryonic death during development, with multiple endothelial and heart defects (65), PC7 knock-out mice were viable and did not exhibit visible anatomical differences (66). Furthermore, other differences between PC7 and Furin began to surface upon analysis of their subcellular localization, which suggested that PC7 concentrates in less dense compartments than Furin (67). Therefore, it was of interest to identify specific PC7 functions, which would differentiate this enzyme from the other PCs and define its nonredundant physiological roles. Pro-EGF processing by PC7 was the first indication of a possible unique processing pathway of PC7. Whether this singular mode of action of PC7 is representative of its general physiological function(s) has yet to be explored in animal models and in human. In this context, we attempted to detect the EGF-115 form in the kidney of PC7 knock-out mice (data not shown). Unfortunately, the available commercial antibodies generated against mature 53-aa EGF (supplemental Fig. S2) do not recognize full-length mouse pro-EGF, and the only commercial mouse pro-EGF antibody (R&D Systems) does not work on Western blot (data not shown). Therefore, a CT-specific mouse pro-EGF antibody would be needed to show the implication of PC7 in pro-EGF processing *in vivo*. In addition, the lack of endogenous PC7-generated EGF-115 production in various cell lines (Neuro2A, HEK293, and β-TC3) that we tested did not allow the use of an effective siRNA approach (supplemental Fig. S3).

What are the domains of PC7 that confer to this enzyme its specific function on pro-EGF? We herein demonstrate that

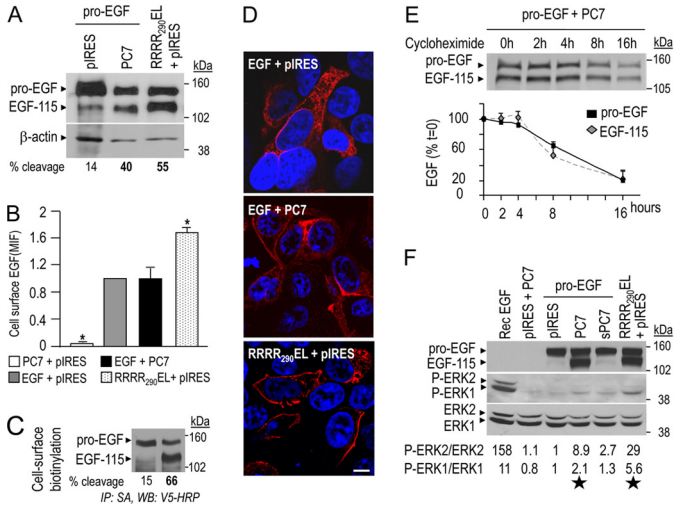

FIGURE 10. **EGF-115 is highly expressed at the cell surface and enhances EGFR activation.** *A,* expression of the pro-EGF-(RRRR^{290}EL) mutant, which is cleaved efficiently by endogenous PCs in HEK293 cells, increases the production of EGF-115, as compared with either pro-EGF + pIRES or co-expressed with PC7. *B,* cell surface EGF immunoreactivity (pro-EGF antibody) obtained by FACS analysis of HEK293 cells expressing PC7, pro-EGF, pro-EGF + PC7, or pro-EGF-(RRRR^{290}EL) shows a clear enrichment of immunoreactivity of the pro-EGF-(RRRR^{290}EL) construct, likely because of the enhanced generation of EGF-115 at the cell surface. The mean intensity of fluorescence (*MIF*) values are plotted as fractions relative to the control sample (EGF + pIRES) for each condition. *Error bars* represent the S.E. for triplicate measurements, and one-way analysis of variance followed by the Dunnett test was used (*, $p < 0.05$). *C,* cell-surface biotinylation of pro-EGF in HEK293 cells co-transfected with pro-EGF and either pIRES or PC7. Proteins were immunoprecipitated (*IP*) with streptavidin-agarose (*SA*) and analyzed by Western blotting (*WB*) using mAb V5-HRP. *D,* cell surface immunofluorescence of pro-EGF in cells expressing pro-EGF, pro-EGF + PC7 or pro-EGF-(*RRRR$_{290}$EL*) (*red labeling*) under slightly permeabilized cells, showing an increased staining at the cell surface in cells expressing pro-EGF-(RRRR^{290}EL). Nuclei of transfected cells were marked by Hoechst 33258 staining (*blue labeling*). *Bar,* 10 μm. *E,* half-life of pro-EGF and EGF-115 measured by Western blotting using mAb V5 after incubation of HEK293 cells expressing pro-EGF + PC7 with 10 μM cycloheximide for 2, 4, 8, and 16 h. The signal intensities are plotted as percentage of control samples ($t = 0$). *Error bars* represent the S.E. for triplicate measurements. *F,* co-cultures of A431 cells, which express high levels of EGFR, with HEK293 cells in the presence of 20 ng of mouse recombinant 53-aa EGF (*Rec EGF*) or HEK293 cells co-expressing pIRES + PC7, or pro-EGF and either pIRES, PC7, or sPC7, pIRES + pro-EGF-(RRRR^{290}EL). Western blot analysis of pro-EGF with mAb V5, compared with that of phosphorylated (*P-*) and nonphosphorylated ERK1/2 revealed that the generation of EGF-115 correlates with an induction of phosphorylation of ERK1/2 as quantitated at the *bottom* of the figure. The ratio of P-ERK/ERK was estimated by Scion image analysis and normalized to that obtained using pIRES + pro-EGF (value = 1). This is a representative example of an experiment repeated at least three times with consistently similar result. *Stars* point out on the increase of ERK1/2 phosphorylation. The percent of pro-EGF cleavage into EGF-115 is indicated *below* each lane.

whereas the transmembrane domain of pro-EGF is dispensable for its processing by PC7 (Fig. 5*A*), anchorage of PC7 to the membrane is indispensable for its activity. To better understand the specificity of PC7 on pro-EGF processing, we examined the effect of post-translational modification of its cytosolic tail. Previously, Cys-palmitoylation of PC7 was reported to stabilize the enzyme without affecting its subcellular localization (58). Our data further show that the nonpalmitoylated PC7-(C699A,C704A) mutant (41) is as active on pro-EGF processing as the WT enzyme, and 2-bromopalmitate does not prevent pro-EGF processing (Fig. 6). These data demonstrate that Cys-palmitoylation does not regulate PC7 activity. Although the TMCT of PC7 is not dispensable, it can be replaced by that of Furin, at least for pro-EGF processing (Figs. 5*B* and 7*B*). In contrast, WT Furin or its PC7 chimeras cannot process pro-EGF (Fig. 7*B*). We conclude that because PC7 does not enhance the cleavage of pro-EGF (Fig. 5*B*), but PC7 activates the cleavage of both pro-EGF and its soluble pro-EGF forms (Fig. 5*A*), the production of EGF-115 requires the TMCT domain of PC7 but not that of pro-EGF. However, the fact that the TMCT of PC7 can be replaced by that of Furin, which is well known to be required for endocytosis of its cognate enzyme (14), also suggests that not just endocytosis is critical but that PC7 possesses specific catalytic properties to generate EGF-115 via its unique ability to activate a presumably latent proteinase.

Attempts to identify the PC7-enhanced cleavage site in pro-EGF were fraught with difficulties in view of the sensitivity of the folding of this protein to domain deletions and the presence of Gln within the N-terminal sequence of the EGF-115 product that blocked its Edman degradation. Nevertheless, combining two mutations, Q292M and K300M, allowed the identification of the cleavage site as Arg$^{290}\downarrow$ within the sequence MVVHPR$^{290}\downarrow$AQ (Fig. 8*C*). We suspected that this processing may not be performed by PC7 but rather by a PC7-activated latent intracellular protease because this motif is not a typical PC-cleavage motif (13). Indeed, the basic aa-specific PC7 still enhanced the processing of the pro-EGF mutant R290A (Fig. 8*D*), and pure soluble PC7 was not active *in vitro* on immunopurified pro-EGF (supplemental Fig. S5*A*) or when incubated with cells expressing pro-EGF at the cell surface (supplemental Fig. S5*B*). We conclude that the production of EGF-115 is performed by a PC7-activated proteinase, expressed in both HEK293 and Neuro2A cells, but much less so in COS-1 cells (Fig. 1*A*). The hypothesis of an indirect cleavage was supported from inhibitory studies whereby the blockade of EGF-115 production was achieved by a cysteine (E64d) and two serine protease (AEBSF and α_1-antitrypsin) inhibitors (Fig. 9*A*), which do not inactivate PC7 *in vitro* (Fig. 9*B*). The protein α_1-antitrypsin is the major inhibitor of neutrophil elastase and proteinase 3 (68, 69), and it has been shown to also inhibit the type II transmembrane serine protease matriptase (70). Because matriptase-2 is expressed in kidney (71) and is processed at multiple Arg residues (72), this raises the possibility that latent matriptase-2 (also known as TMPRSS6), or a functional homologue, may be a potential candidate for activation by PC7, resulting in pro-EGF processing. Finally, we do not believe that the cognate enzyme activity requires a glycosylphosphatidylinositol-anchored cell-surface enzyme, like kidney prostasin (73), because production of EGF-115 was not affected by treatment of cells with phospholipase C (Fig. 9*C*).

We next demonstrated that processing occurs in a lipid-rich post-ER compartment and requires endocytosis from clathrin-coated-pits of either pro-EGF, PC7, and/or the latent enzyme(s) to generate EGF-115 (Fig. 4*F*). However cleavage of pro-EGF does not require an acidic compartment, because incubation of cells with 5 mM NH_4Cl had no effect on its processing (data not shown). Therefore, although the cleavage site of pro-EGF and the class of the intermediate enzyme(s) have been identified, the specific enzyme(s) and subcellular localization of the PC7-activated processing reaction remain elusive.

Although mature EGF can effectively bind and activate the EGFR, the membrane-bound and shed EGF forms are also

potent activators of this pathway (11, 74–76). The pro-EGF mutant RRRR^{290}EL, which is very efficiently processed by endogenous PCs in HEK293 cells into the EGF-115 (Fig. 10*A*), is more active than wild type EGF in stimulating the EGFR pathway, as evidenced by the increased levels of phospho-ERK1/2 (Fig. 10*F*). Our data suggest that activation of the EGFR is due to the presence of a high level of EGF-115 at the cell surface (Fig. 10*C*) rather than its higher ability to activate its receptor. We obtained very similar results with a RRRR^{315}EL mutant of pro-EGF (data not shown), suggesting that cleavage of pro-EGF between aa 290 or 315 increases the activity of the remaining product through its enhanced cell surface localization.

Intriguingly, the biosynthetic pathway of pro-EGF maturation into different intermediate soluble and transmembrane forms has not been studied in detail (77–79). The cytoplasmic domain of pro-EGF has been described to have its intrinsic biological activity. For example, it negatively modulates the regulation of motility and elastinolytic invasion in human thyroid cancer cells (80) and induces a reduction in body and organ weights in transgenic mice, including smaller kidney and brain (81). In contrast, the role of the extracellular region of mouse pro-EGF, which contains nine EGF-like domains and eight LDL receptor class B repeats (82), has not been defined. Furthermore, no previous work addressed the functional role of aa 26–290 of pro-EGF, a domain removed by the PC7-activated protease in our study. Because cleavage of this domain enhanced the cell surface localization of EGF-115, and its activity on EGFR, we presume that the presence of this N-terminal sequence is a negative modulator of pro-EGF cell surface localization, either by a conformational effect or through binding to an intracellular partner. Conceptually, because pro-EGF processing requires endocytosis into clathrin-coated vesicles (Fig. 4*F*), the N-terminal domain of pro-EGF may prevent its recycling to the cell surface. Hence, processing would release the N-terminal domain and result in EGF-115 as the major pro-EGF form at the cell surface (Fig. 10*C*).

In conclusion, our present data show the uniqueness of the ability of PC7 to enhance pro-EGF processing into EGF-115, which is found in the kidney but not in lacrimal glands, upon prior activation of a latent serine and/or cysteine protease(s). The data also suggest that the PC7-induced generation of EGF-115 may represent a regulatory mechanism of juxtacrine EGFR activation, at least in kidney.

Acknowledgments—We are grateful to Josée Hamelin for excellent technical assistance and Dany Gauthier for microsequencing experiment. We also thank Dr. Annik Prat for valuable advice. We also thank all the members of the Seidah laboratory for helpful discussions and Brigitte Mary for efficacious editorial assistance.

REFERENCES

1. Scott, J., Patterson, S., Rall, L., Bell, G. I., Crawford, R., Penschow, J., Niall, H., and Coghlan, J. (1985) *J. Cell Sci. Suppl.* **3,** 19–28
2. Schneider, M. R., and Wolf, E. (2009) *J. Cell. Physiol.* **218,** 460–466
3. King, C. R., Borrello, I., Bellot, F., Comoglio, P., and Schlessinger, J. (1988) *EMBO J.* **7,** 1647–1651
4. Stern, D. F., and Kamps, M. P. (1988) *EMBO J.* **7,** 995–1001
5. Grandis, J. R., and Sok, J. C. (2004) *Pharmacol. Ther.* **102,** 37–46
6. Dutta, P. R., and Maity, A. (2007) *Cancer Lett.* **254,** 165–177
7. Jørgensen, P. E., Nexø, E., Poulsen, S. S., Almendingen, M., and Berg, T. (1994) *Growth Factors* **11,** 113–123
8. Jørgensen, E., Nexø, E., and Poulsen, S. S. (1991) *Biochim. Biophys. Acta* **1074,** 284–288
9. Rall, L. B., Scott, J., Bell, G. I., Crawford, R. J., Penschow, J. D., Niall, H. D., and Coghlan, J. P. (1985) *Nature* **313,** 228–231
10. Le Gall, S. M., Meneton, P., Mauduit, P., and Dreux, C. (2004) *Regul. Pept.* **122,** 119–129
11. Breyer, J. A., and Cohen, S. (1990) *J. Biol. Chem.* **265,** 16564–16570
12. Maréchal, H., Jammes, H., Rossignol, B., and Mauduit, P. (1999) *Am. J. Physiol.* **276,** C734–C746
13. Seidah, N. G., and Chrétien, M. (1999) *Brain Res.* **848,** 45–62
14. Thomas, G. (2002) *Nat. Rev. Mol. Cell Biol.* **3,** 753–766
15. Steiner, D. F. (1998) *Curr. Opin. Chem. Biol.* **2,** 31–39
16. Seidah, N. G., Mayer, G., Zaid, A., Rousselet, E., Nassoury, N., Poirier, S., Essalmani, R., and Prat, A. (2008) *Int. J. Biochem. Cell Biol.* **40,** 1111–1125
17. Seidah, N. G., and Prat, A. (2007) *J. Mol. Med.* **85,** 685–696
18. Seidah, N. G., Chrétien, M., and Day, R. (1994) *Biochimie* **76,** 197–209
19. Ben-Haim, N., Lu, C., Guzman-Ayala, M., Pescatore, L., Mesnard, D., Bischofberger, M., Naef, F., Robertson, E. J., and Constam, D. B. (2006) *Dev. Cell* **11,** 313–323
20. Essalmani, R., Zaid, A., Marcinkiewicz, J., Chamberland, A., Pasquato, A., Seidah, N. G., and Prat, A. (2008) *Proc. Natl. Acad. Sci. U.S.A.* **105,** 5750–5755
21. Creemers, J. W., and Khatib, A. M. (2008) *Front. Biosci.* **13,** 4960–4971
22. Basak, A., Zhong, M., Munzer, J. S., Chrétien, M., and Seidah, N. G. (2001) *Biochem. J.* **353,** 537–545
23. Munzer, J. S., Basak, A., Zhong, M., Mamarbachi, A., Hamelin, J., Savaria, D., Lazure, C., Hendy, G. N., Benjannet, S., Chrétien, M., and Seidah, N. G. (1997) *J. Biol. Chem.* **272,** 19672–19681
24. Touré, B. B., Munzer, J. S., Basak, A., Benjannet, S., Rochemont, J., Lazure, C., Chrétien, M., and Seidah, N. G. (2000) *J. Biol. Chem.* **275,** 2349–2358
25. Blais, V., Fugère, M., Denault, J. B., Klarskov, K., Day, R., and Leduc, R. (2002) *FEBS Lett.* **524,** 43–48
26. Siegfried, G., Basak, A., Cromlish, J. A., Benjannet, S., Marcinkiewicz, J., Chrétien, M., Seidah, N. G., and Khatib, A. M. (2003) *J. Clin. Invest.* **111,** 1723–1732
27. Basak, S., Chrétien, M., Mbikay, M., and Basak, A. (2004) *Biochem. J.* **380,** 505–514
28. Scamuffa, N., Basak, A., Lalou, C., Wargnier, A., Marcinkiewicz, J., Siegfried, G., Chrétien, M., Calvo, F., Seidah, N. G., and Khatib, A. M. (2008) *Gut* **57,** 1573–1582
29. Fugere, M., Appel, J., Houghten, R. A., Lindberg, I., and Day, R. (2007) *Mol. Pharmacol.* **71,** 323–332
30. Decroly, E., Wouters, S., Di Bello, C., Lazure, C., Ruysschaert, J. M., and Seidah, N. G. (1996) *J. Biol. Chem.* **271,** 30442–30450
31. Decroly, E., Benjannet, S., Savaria, D., and Seidah, N. G. (1997) *FEBS Lett.* **405,** 68–72
32. van de Loo, J. W., Creemers, J. W., Bright, N. A., Young, B. D., Roebroek, A. J., and Van de Ven, W. J. (1997) *J. Biol. Chem.* **272,** 27116–27123
33. Canaff, L., Bennett, H. P., Hou, Y., Seidah, N. G., and Hendy, G. N. (1999) *Endocrinology* **140,** 3633–3642
34. Lopez-Perez, E., Seidah, N. G., and Checler, F. (1999) *J. Neurochem.* **73,** 2056–2062
35. Zhong, M., Munzer, J. S., Basak, A., Benjannet, S., Mowla, S. J., Decroly, E., Chrétien, M., and Seidah, N. G. (1999) *J. Biol. Chem.* **274,** 33913–33920
36. McColl, B. K., Paavonen, K., Karnezis, T., Harris, N. C., Davydova, N., Rothacker, J., Nice, E. C., Harder, K. W., Roufail, S., Hibbs, M. L., Rogers, P. A., Alitalo, K., Stacker, S. A., and Achen, M. G. (2007) *FASEB J.* **21,** 1088–1098
37. Longpré, J. M., McCulloch, D. R., Koo, B. H., Alexander, J. P., Apte, S. S., and Leduc, R. (2009) *Int. J Biochem. Cell Biol.* **41,** 1116–1126
38. Nelsen, S. M., and Christian, J. L. (2009) *J. Biol. Chem.* **284,** 27157–27166
39. Khatib, A. M., Lahlil, R., Scamuffa, N., Akimenko, M. A., Ernest, S., Lomri, A., Lalou, C., Seidah, N. G., Villoutreix, B. O., Calvo, F., and Siegfried, G. (2010) *PLoS ONE* **5,** e11438
40. Seidah, N. G., Hamelin, J., Mamarbachi, M., Dong, W., Tardos, H., Mbi-

kay, M., Chretien, M., and Day, R. (1996) *Proc. Natl. Acad. Sci. U.S.A.* **93,** 3388–3393
41. Rousselet, E., Benjannet, S., Hamelin, J., Canuel, M., and Seidah, N. G. (2011) *J. Biol. Chem.* **286,** 2728–2738
42. Ozden, S., Lucas-Hourani, M., Ceccaldi, P. E., Basak, A., Valentine, M., Benjannet, S., Hamelin, J., Jacob, Y., Mamchaoui, K., Mouly, V., Desprès, P., Gessain, A., Butler-Browne, G., Chrétien, M., Tangy, F., Vidalain, P. O., and Seidah, N. G. (2008) *J. Biol. Chem.* **283,** 21899–21908
43. Seidah, N. G., Benjannet, S., Wickham, L., Marcinkiewicz, J., Jasmin, S. B., Stifani, S., Basak, A., Prat, A., and Chretien, M. (2003) *Proc. Natl. Acad. Sci. U.S.A.* **100,** 928–933
44. Benjannet, S., Reudelhuber, T., Mercure, C., Rondeau, N., Chrétien, M., and Seidah, N. G. (1992) *J. Biol. Chem.* **267,** 11417–11423
45. Benjannet, S., Elagoz, A., Wickham, L., Mamarbachi, M., Munzer, J. S., Basak, A., Lazure, C., Cromlish, J. A., Sisodia, S., Checler, F., Chrétien, M., and Seidah, N. G. (2001) *J. Biol. Chem.* **276,** 10879–10887
46. Okada, T., Haze, K., Nadanaka, S., Yoshida, H., Seidah, N. G., Hirano, Y., Sato, R., Negishi, M., and Mori, K. (2003) *J. Biol. Chem.* **278,** 31024–31032
47. Pullikotil, P., Vincent, M., Nichol, S. T., and Seidah, N. G. (2004) *J. Biol. Chem.* **279,** 17338–17347
48. Tofighi, R., Tillmark, N., Daré, E., Aberg, A. M., Larsson, J. E., and Ceccatelli, S. (2006) *Brain Res.* **1098,** 1–8
49. Zelvyte, I., Stevens, T., Westin, U., and Janciauskiene, S. (2004) *Cancer Cell Int.* **4,** 7
50. Iwashita, K., Kitamura, K., Narikiyo, T., Adachi, M., Shiraishi, N., Miyoshi, T., Nagano, J., Tuyen, D. G., Nonoguchi, H., and Tomita, K. (2003) *J. Am. Soc. Nephrol.* **14,** 11–16
51. Mansell, A., Reinicke, A., Worrall, D. M., and O'Neill, L. A. (2001) *FEBS Lett.* **508,** 313–317
52. Mishima, Y., Terui, Y., Sugimura, N., Matsumoto-Mishima, Y., Rokudai, A., Kuniyoshi, R., and Hatake, K. (2007) *Cancer Sci.* **98,** 364–372
53. Mentlein, R., and Dahms, P. (1994) *J. Neurochem.* **62,** 27–36
54. Lippincott-Schwartz, J., Yuan, L., Tipper, C., Amherdt, M., Orci, L., and Klausner, R. D. (1991) *Cell* **67,** 601–616
55. Scheel, A. A., and Pelham, H. R. (1996) *Biochemistry* **35,** 10203–10209
56. Kilsdonk, E. P., Yancey, P. G., Stoudt, G. W., Bangerter, F. W., Johnson, W. J., Phillips, M. C., and Rothblat, G. H. (1995) *J. Biol. Chem.* **270,** 17250–17256
57. Macia, E., Ehrlich, M., Massol, R., Boucrot, E., Brunner, C., and Kirchhausen, T. (2006) *Dev. Cell* **10,** 839–850
58. van de Loo, J. W., Teuchert, M., Pauli, I., Plets, E., Van de Ven, W. J., and Creemers, J. W. (2000) *Biochem. J.* **352,** 827–833
59. Djie, M. Z., Le Bonniec, B. F., Hopkins, P. C., Hipler, K., and Stone, S. R. (1996) *Biochemistry* **35,** 11461–11469
60. Mahrus, S., Kisiel, W., and Craik, C. S. (2004) *J. Biol. Chem.* **279,** 54275–54282
61. Benjannet, S., Rhainds, D., Hamelin, J., Nassoury, N., and Seidah, N. G. (2006) *J. Biol. Chem.* **281,** 30561–30572
62. Glading, A., Chang, P., Lauffenburger, D. A., and Wells, A. (2000) *J. Biol. Chem.* **275,** 2390–2398
63. King, I. C., and Sartorelli, A. C. (1986) *Biochem. Biophys. Res. Commun.* **140,** 837–843
64. Meerabux, J., Yaspo, M. L., Roebroek, A. J., Van de Ven, W. J., Lister, T. A., and Young, B. D. (1996) *Cancer Res.* **56,** 448–451
65. Roebroek, A. J., Umans, L., Pauli, I. G., Robertson, E. J., van Leuven, F., Van de Ven, W. J., and Constam, D. B. (1998) *Development* **125,** 4863–4876
66. Villeneuve, P., Feliciangeli, S., Croissandeau, G., Seidah, N. G., Mbikay, M., Kitabgi, P., and Beaudet, A. (2002) *J. Neurochem.* **82,** 783–793
67. Wouters, S., Decroly, E., Vandenbranden, M., Shober, D., Fuchs, R., Morel, V., Leruth, M., Seidah, N. G., Courtoy, P. J., and Ruysschaert, J. M. (1999) *FEBS Lett.* **456,** 97–102
68. Potempa, J., Korzus, E., and Travis, J. (1994) *J. Biol. Chem.* **269,** 15957–15960
69. Geraghty, P., Rogan, M. P., Greene, C. M., Brantly, M. L., O'Neill, S. J., Taggart, C. C., and McElvaney, N. G. (2008) *Thorax* **63,** 621–626
70. Janciauskiene, S., Nita, I., Subramaniyam, D., Li, Q., Lancaster, J. R., Jr., and Matalon, S. (2008) *Am. J. Respir. Cell Mol. Biol.* **39,** 631–637
71. Hooper, J. D., Campagnolo, L., Goodarzi, G., Truong, T. N., Stuhlmann, H., and Quigley, J. P. (2003) *Biochem. J.* **373,** 689–702
72. Stirnberg, M., Maurer, E., Horstmeyer, A., Kolp, S., Frank, S., Bald, T., Arenz, K., Janzer, A., Prager, K., Wunderlich, P., Walter, J., and Gütschow, M. (2010) *Biochem. J.* **430,** 87–95
73. Svenningsen, P., Uhrenholt, T. R., Palarasah, Y., Skjødt, K., Jensen, B. L., and Skøtt, O. (2009) *Am. J. Physiol. Regul. Integr. Comp. Physiol.* **297,** R1733–R1741
74. Mroczkowski, B., Reich, M., Chen, K., Bell, G. I., and Cohen, S. (1989) *Mol. Cell. Biol.* **9,** 2771–2778
75. Parries, G., Chen, K., Misono, K. S., and Cohen, S. (1995) *J. Biol. Chem.* **270,** 27954–27960
76. Kwan, R. W., Wong, R. W., and Chan, S. Y. (1999) *Int. J. Oncol.* **15,** 281–284
77. Frey, P., Forand, R., Maciag, T., and Shooter, E. M. (1979) *Proc. Natl. Acad. Sci. U.S.A.* **76,** 6294–6298
78. Raab, G., Higashiyama, S., Hetelekidis, S., Abraham, J. A., Damm, D., Ono, M., and Klagsbrun, M. (1994) *Biochem. Biophys. Res. Commun.* **204,** 592–597
79. Journe, F., Wattiez, R., Piron, A., Carion, M., Laurent, G., Heuson-Stiennon, J. A., and Falmagne, P. (1997) *Biochim. Biophys. Acta* **1357,** 18–30
80. Glogowska, A., Pyka, J., Kehlen, A., Los, M., Perumal, P., Weber, E., Cheng, S. Y., Hoang-Vu, C., and Klonisch, T. (2008) *Neoplasia* **10,** 1120–1130
81. Klonisch, T., Glogowska, A., Gratao, A. A., Grzech, M., Nistor, A., Torchia, M., Weber, E., de Angelis, M. H., Rathkolb, B., Cuong, H. V., Wolf, E., and Schneider, M. R. (2009) *FEBS Lett.* **583,** 1349–1357
82. Valcarce, C., Björk, I., and Stenflo, J. (1999) *Eur. J. Biochem.* **260,** 200–207